Molecular Therapy
Nucleic Acids
Original Article

Validation of Gene Therapy for Mutant Mitochondria by Delivering Mitochondrial RNA Using a MITO-Porter

Eriko Kawamura,[1,6] Minako Maruyama,[1] Jiro Abe,[2] Akira Sudo,[3,4] Atsuhito Takeda,[2] Shingo Takada,[5] Takashi Yokota,[5] Shintaro Kinugawa,[5] Hideyoshi Harashima,[1] and Yuma Yamada[1,6]

[1]Faculty of Pharmaceutical Sciences, Hokkaido University, Kita-12, Nishi-6, Kita-ku, Sapporo 060-0812, Japan; [2]Department of Pediatrics, Hokkaido University Hospital, Kita-15, Nishi-7, Kita-ku, Sapporo 060-8638, Japan; [3]Nire-no-kai Children's Clinic, Atsubetsu-cho Shimonopporo-49, Atsubetsu-ku, Sapporo 004-0007, Japan; [4]Department of Pediatrics, Sapporo City General Hospital, Kita-11, Nishi-13, Chuo-ku, Sapporo 060-8604, Japan; [5]Department of Cardiovascular Medicine, Graduate School of Medicine, Hokkaido University, Kita-15, Nishi-7, Kita-ku, Sapporo 060-8638, Japan

Here, we report on validating a mitochondrial gene therapy by delivering nucleic acids to mitochondria of diseased cells by a MITO-Porter, a liposome-based carrier for mitochondrial delivery. We used cells derived from a patient with a mitochondrial disease with a G625A heteroplasmic mutation in the tRNA^{Phe} of the mitochondrial DNA (mtDNA). It has been reported that some mitochondrial gene diseases are caused by heteroplasmic mutations, in which both mutated and wild-type (WT) genes are present, and the accumulation of pathological mutations leads to serious, intractable, multi-organ diseases. Therefore, the decrease of the mutated gene rate is considered to be a useful gene therapy strategy. To accomplish this, wild-type mitochondrial pre-tRNA^{Phe} (pre-WT-tRNA^{Phe}), prepared by *in vitro* transcription, was encapsulated in the MITO-Porter. The pre-WT-tRNA^{Phe} encapsulated in the MITO-Porter was transfected into diseased mitochondrial cells, and the resulting mutant levels were examined by an amplification refractory mutation system (ARMS)-quantitative PCR. The mutation rate of tRNA^{Phe} was decreased, and this therapeutic effect was sustained even on the 8th day after transfection. Furthermore, mitochondrial respiratory activity of the disease cells was increased after the transfection of therapeutic pre-WT-tRNA^{Phe}. These results support the conclusion that the mitochondrial delivery of therapeutic nucleic acids represents a viable strategy for mitochondrial gene therapy.

INTRODUCTION

There are multiple mitochondrial DNAs (mtDNAs) in mitochondria, with several thousand copies of mtDNA contained in one cell.[1] Furthermore, it has been reported that in fibroblasts, one cell contains about 800 nucleoids, in which 2 to 3 mtDNAs are condensed with a set of DNA-binding core proteins that are involved in mtDNA maintenance and transcription.[2] Mitochondrial gene diseases are classified into homoplasmic mutations in which only mutant mtDNA exists and heteroplasmic mutations in which mutated mtDNA and normal mtDNA coexist. In the case of heteroplasmic mutations, it has been reported that when the mutation rate of mtDNA exceeds a certain threshold value, disease symptoms associated with mitochondrial function decline in development.[3,4]

In this study, to validate a mitochondrial gene therapeutic strategy using cells derived from mitochondrial disease patients, primary cultured skin fibroblasts, obtained from a skin biopsy of a patient with a mutation in mitochondrial tRNA^{Phe} (Figure 1), were examined. The mitochondria of the patient had a heteroplasmic mutation of G625A in tRNA^{Phe}, and it has been reported that the mutation rate for this is about 80%.[5] The clinical symptoms for this mutation include progressive hearing impairment, epilepsy, and elevated lactic acid levels. Our objective in this study was to verify a mitochondrial gene-therapy strategy using cells derived from this mitochondrial disease patient.

In an attempt to develop a mitochondrial gene therapy, Karicheva et al.[6] reported on a therapeutic method that involved a tRNA mutation to tRNA$^{Leu\ (UUR)}$, a A3243G mutation. In that study, wild-type (WT) RNA was transported to mitochondria via allotropic expression, a method for transfecting plasmid DNA (pDNA) encoding an RNA/protein with a mitochondrial targeting signal into the nucleus and delivering the nuclear-expressed RNA or protein to mitochondria (Figure 2Aa). The authors expressed the mimic tRNA$^{Leu\ (UUR)}$ in the nucleus and delivered the tRNA to mitochondria. As a result, the level of expression of mitochondrial proteins increased, and mitochondrial respiratory capacity was recovered. However, this strategy, which is based on allotropic expression, would be expected to overcome many procedures, including nuclear gene transfer, gene expression, and mitochondrial delivery from the cytoplasm.

Received 24 February 2020; accepted 15 April 2020;
https://doi.org/10.1016/j.omtn.2020.04.004.

[6]These authors contributed equally to this work.

Correspondence: Yuma Yamada, Faculty of Pharmaceutical Sciences, Hokkaido University, Kita-12, Nishi-6, Kita-ku, Sapporo 060-0812, Japan.
E-mail: u-ma@pharm.hokudai.ac.jp

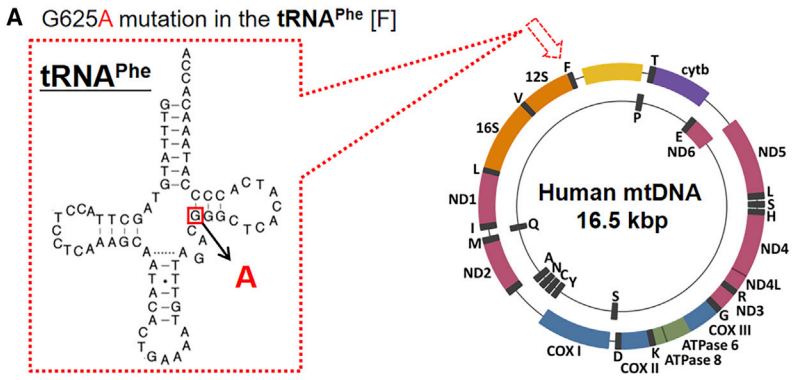

Figure 1. Overview of Mitochondrial Cells from the Disease Patient (G625A Fibroblasts) Used in This Study

G625A fibroblasts have a G625A heteroplasmic mutation in the tRNA^{Phe} of mtDNA. (A) The G625A mutation is located on the variable loop from the T loop of tRNA^{Phe}. (B) Observations of G625A fibroblasts after staining mitochondria with MitoTracker Deep Red (red color) and Rhodamine 123 (green color). MitoTracker Deep Red stains mitochondria even when membrane potential is lost, whereas Rhodamine 123 is dependent on the membrane potential. The cells were observed using CLSM. Scale bars, 20 μm.

To date, the transport of several RNA sequences from the cytoplasm to mitochondria has been reported.[7–9] However, it has been shown that RNA is not transported to mitochondria by itself, and a cytosolic endogenous protein for mitochondrial transport is required. Since the level of expression of this protein is rate limiting, the efficiency of transport to mitochondria is a very low level. In order to transport much larger amounts of RNA to mitochondria, a MITO-Porter, a liposome-based carrier for the mitochondrial delivery, was developed in our laboratory,[10–16] and was found to be a useful strategy. The MITO-Porter is internalized into cells and delivers encapsulated molecules to mitochondria via membrane fusion, a process that is independent of its size and physical properties. Therefore, this system could be used for the direct mitochondrial transfection of nucleic acids.

In this study, we attempted to deliver wild-type mitochondrial pre-tRNA^{Phe} (pre-WT-tRNA^{Phe}) using a MITO-Porter in an attempt to decrease the mutation rate of tRNA^{Phe} in mitochondria in a mitochondrial disease cell with a G625A heteroplasmic mutation in the tRNA^{Phe} of mtDNA (Figure 2Ab). The resulting mutant levels were examined by an amplification refractory mutation system (ARMS)-quantitative PCR. We also investigated the influence of this on the mitochondrial respiratory activity associated with the decrease in the mutation rate.

RESULTS

A Mitochondrial Gene Therapeutic Strategy for Targeting Mutant Mitochondria and the Design of a pDNA to Express Therapeutic tRNA

As a therapeutic strategy for targeting mutant mitochondria, we attempted to deliver pre-WT-tRNA^{Phe} using a MITO-Porter in order to decrease the mutant level of tRNA^{Phe} in mitochondria, followed by improving mitochondrial activity (Figure 2Ab). In addition, we compared the heteroplasmy levels of tRNA^{Phe} after the mitochondrial delivery of the tRNA via a MITO-Porter system and an allotropic expression system. The allotropic expression used in this study is a method for transfecting pDNA encoding the tRNA^{Phe} with a mitochondrial targeting signal into the nucleus and delivering the resulting nuclear-expressed tRNA^{Phe} to mitochondria (Figure 2Aa).

We first designed a pDNA encoding pre-WT-tRNA^{Phe} to validate our therapeutic strategy using a mitochondrial disease cell with a G625A heteroplasmic mutation in the tRNA^{Phe}. In order for tRNA to function in mitochondria, various processes to convert it from pre-tRNA to mature tRNA, including modification of a number of bases, the addition of a 3′ terminal CCA, and aminoacylation, are needed. It is well known that these processes occur in the pre-tRNA state during its transcription from mtDNA. Thus, even if the sequence of tRNA without an untranslated region (UTR) synthesized by *in vitro* transcription could be delivered to mitochondria, the tRNA sequence could not function in mitochondria as an adaptor molecule for protein synthesis.[6] From this, we designed pre-WT-tRNA^{Phe} by mimicking pre-tRNA to which ten bases of 5′ and 3′ terminal sequences were added.

The designs of the pDNA vectors used in this study are shown in Figure 2B. pT7-WT-tRNA^{Phe} was designed by inserting a DNA fragment containing the T7 promoter and the wild-type tRNA^{Phe} gene with the 5′ and 3′ UTR (Vector Sequence S1) into the pUC57-Amp vector between the multi-cloning site (EcoRI and BglII sites) (Figure 2Ba). DNA fragments, including RNaseP RNA (RP)-WT-tRNA^{Phe}-mitochondrial ribosomal protein (MRP) (Figure 2Bb; Vector Sequence S2), tRK1-WT-tRNA^{Phe} (Figure 2Bc; Vector Sequence S3), and tRNA^{Phe} (yeast) as a negative control (Figure 2Bd; Vector Sequence S4), are shown. RNAs for loading into the MITO-Porter were prepared as templates of pDNA with the T7 promoter via an *in vitro* transcription system, including T7 RNA polymerase.

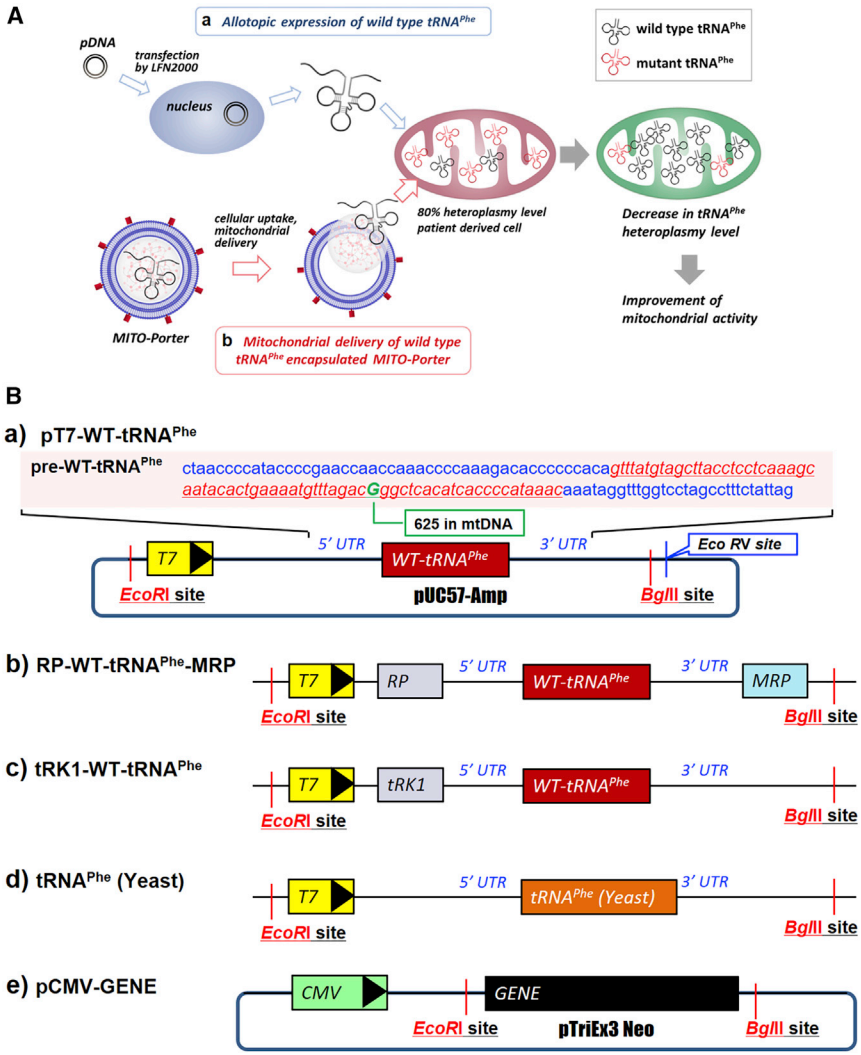

Figure 2. Schematic Images of Our Strategy for Mitochondrial Gene Therapy Targeting Mutant Mitochondria and the Design of the pDNA Vectors

(A) As a therapeutic strategy targeting mutant mitochondria, WT-tRNA^{Phe} is delivered to mitochondria of G625A fibroblasts in order to decrease the mutant level of tRNA^{Phe} in mitochondria via an allotropic expression system (a) or a MITO-Porter system (b). (B) The designs of pDNAs, where DNA fragments are inserted into the pUC57-Amp vector or pTriEx3 Neo vector with the CMV promoter (EcoRI and BglII sites), are shown. pT7-WT-tRNA^{Phe} was designed by inserting the DNA fragment containing the T7 promoter and wild-type tRNA^{Phe} gene with the 5′ and 3′ UTR (Vector Sequence S1) into the pUC57-Amp vector without a promoter (a). DNA fragments, including RP-WT-tRNA^{Phe}-MRP (b; Vector Sequence S2), tRK1-WT-tRNA^{Phe} (c; Vector Sequence S3), and tRNA^{Phe} (yeast) (d; Vector Sequence S4), are shown. (e) Structure of pDNA constructed using the pTriEx3 Neo vector with the CMV promoter.

For allotropic expression, we designed pDNA with the cytomegalovirus (CMV) promoter to produce nuclear-expressed tRNA^{Phe} (Figure 2Be). RP-WT-tRNA^{Phe}-MRP contains RP and MRP sequences that are reported to function as a mitochondrial import signal of RNA.[17] tRK1-WT-tRNA^{Phe} contains yeast tRNA Lys (CTT) (tRK1 sequence) with mitochondrial import activity.[6] Thus, it was expected that transfection of pCMV-RP-WT-tRNA^{Phe}-MRP and pCMV-tRK1-WT-tRNA^{Phe} into the nucleus would permit the mitochondrial delivery of nuclear-expressed tRNA^{Phe}. In addition, these mitochondrial import signals might support direct mitochondrial transfection using a MITO-Porter.

Construction of MITO-Porter Encapsulating Therapeutic tRNA

Before beginning to validate the mitochondrial gene therapeutic strategy using G625A fibroblasts, the mitochondrial function of the cells was evaluated by observing mitochondrial membrane potentials. As shown in Figure 1B, the mitochondria in G625A fibroblasts were stained with MitoTracker Deep Red and Rhodamine 123, followed by the intracellular observation by confocal laser-scanning microscopy (CLSM). MitoTracker Deep Red (red color) is able to stain mitochondria, even when membrane potential is lost, whereas Rhodamine 123 (green color) is dependent on the mitochondrial membrane potential. Our findings indicate that these mitochondrial morphologies were similar to those from normal cells (Figure 1Ba) and that only a few mitochondria were stained with Rhodamine 123 (Figure 1Bb), suggesting that the mitochondrial membrane potentials were low.

To validate whether MITO-Porter envelops could be internalized into G625A fibroblasts and reach mitochondria, we observed intracellular localization of the empty MITO-Porter labeled with a fluorescent dye (green color) after staining the mitochondria red with CLSM (Figure 3A). The green-colored MITO-Porters were internalized into the cells, and some were eventually localized with mitochondria and observed as yellow signals. This result suggests that this MITO-Porter system could be used to deliver cargoes to mitochondria of G625A fibroblasts.

We next attempted to package the purified therapeutic RNA (pre-WT-tRNA^{Phe}) in the MITO-Porter, as shown in Figure 3B. The preparation of the MITO-Porter encapsulating nanoparticles of pre-WT-tRNA^{Phe} requires the following steps: (1) formation of a nanoparticle of pre-WT-tRNA^{Phe} with a polycation (protamine) via electrostatic interactions and (2) packaging of the nanoparticle of pre-WT-tRNA^{Phe} with a mitochondrial fusogenic lipid envelope, followed by modification with the octa-arginine (R8) peptide (a cellular uptake and mitochondrial targeting device).[18–20]

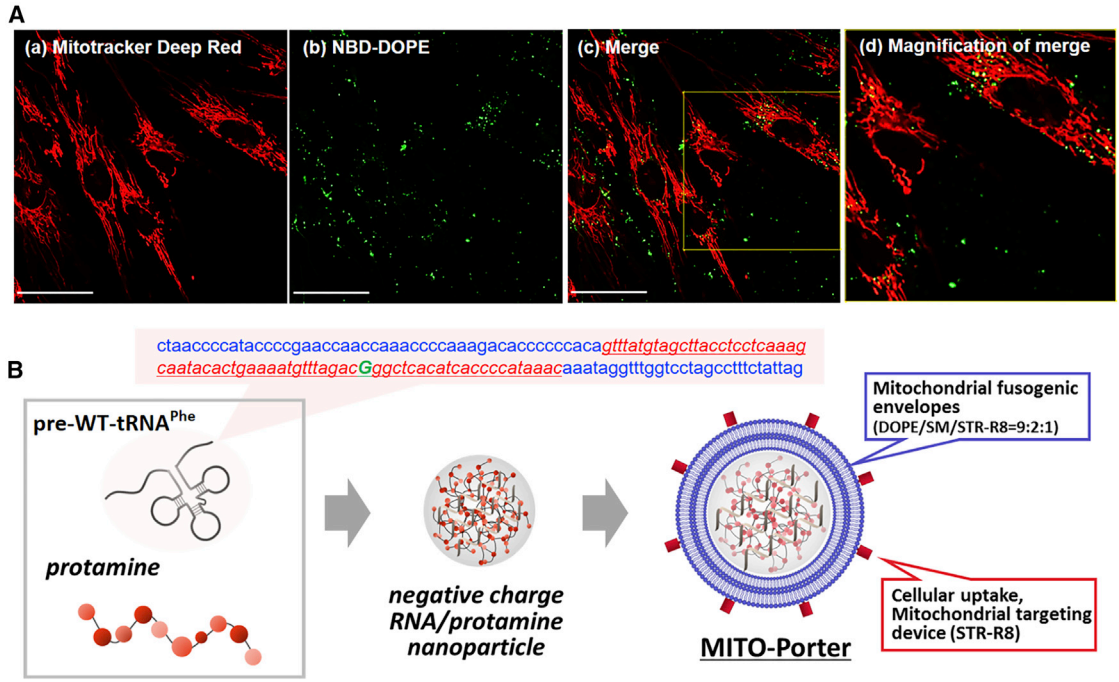

Figure 3. Intracellular Localization of the MITO-Porter in G625A Fibroblasts and the Packaging of Therapeutic RNA in the MITO-Porter

(A) Intracellular observations of MITO-Porter in G625A fibroblasts. G625A fibroblasts were incubated with the MITO-Porter labeled with NBD-DOPE (a green fluorescence lipid). After staining the mitochondria red with MitoTracker Deep Red, the cells were observed by CLSM (a) image of MitoTracker Deep Red; (b) image of NBD-DOPE; (c) merge image; and (d) magnification of merge image. NBD-labeled MITO-Porter appeared as yellow clusters when it was localized in mitochondria. Scale bars, 50 μm. (B) Schematic illustration of the construction of the MITO-Porter (WT-tRNA^{Phe}). The construction of the MITO-Porter encapsulating nanoparticles of WT-tRNA^{Phe} requires the following steps: (1) formation of a nanoparticle of WT-tRNA^{Phe} with a polycation (protamine) via electrostatic interactions and (2) packaging of the nanoparticle of WT-tRNA^{Phe} with a mitochondrial fusogenic lipid envelope, followed by modification of the R8 peptide (a cellular uptake and mitochondrial targeting device) to the carrier.

As a first step, a solution of pre-WT-tRNA^{Phe} was mixed with a protamine to form a nanoparticle of pre-WT-tRNA^{Phe}. It has been reported that protamine functions as a pDNA condensing element[21,22] and easily releases nucleic acids via a high response activity to anion molecules in cells. In this study, we used small, negatively charged particles formed at a nitrogen/phosphate (N/P) ratio of 0.9 for preparing the MITO-Porter (WT-tRNA^{Phe}). The diameter, polydispersity index (PDI; an indicator of particle-size distribution), and ζ potential of the nanoparticles were 122 ± 12 nm, 0.143 ± 0.040, and −31 ± 8 mV, respectively (n = 5).

The resulting negatively charged nanoparticles were then packaged in cationic lipid envelopes by the ethanol dilution method to produce the MITO-Porter (WT-tRNA^{Phe}). We also prepared a MITO-Porter encapsulating RP-WT-tRNA^{Phe}-MRP, tRK1-WT-tRNA^{Phe}, or tRNA^{Phe} (yeast) to produce MITO-Porter (RP-WT-tRNA^{Phe}-MRP), MITO-Porter (tRK1-WT-tRNA^{Phe}), or MITO-Porter (tRNA^{Phe} (yeast)). The physicochemical properties of the prepared carriers, which are listed in Table 1, show that carriers with diameters of less than 200 nm could be prepared with a highly homogeneous composition (PDI value of less than 0.20). The ζ potential of the carriers was ~40 mV.

Establishment to Evaluate the Mutation Rate of tRNA^{Phe} in Mitochondria

As shown in Figure 4A, the mutation rate of the tRNA^{Phe} extracted from mitochondria of disease cells was determined using the ARMS-PCR method. As a first step, therapeutic RNA was transfected into diseased cells with the MITO-Porter (step 1), and the cells were then washed with CellScrub buffer in order to remove MITO-Porter bound to the surface of cell membranes (step 2). CellScrub buffer is a commercially available reagent that is used to remove positive-charged particles bound to cellular membranes. In the next step, the cells were homogenized using a syringe needle, and the fraction containing nuclei and fracted cells were removed by centrifugation (step 3). In order to remove tRNA^{Phe} that was located outside the mitochondria, the resulting fraction was incubated with RNase (step 4), and mitochondria were isolated by density gradient centrifugation (step 5). In the final step, total RNAs were extracted from the isolated mitochondria (step 6), cDNAs were prepared using a reverse transcription reaction (step 7), and ARMS-PCR was then used for the quantitative determination of the rate of mutation of G625A (step 8).

The ARMS-PCR method is generally used to detect mutations in genes and has recently been used as a method for detecting the mutation rate of mtDNA.[23] In this experiment, reverse primers were

Table 1. Physicochemical Properties of MITO-Porter Encapsulating Various Types of Pre-tRNA^{Phe}

Encapsulated RNA	Diameters (nm)	PDI	ζ Potential (mV)
Pre-WT-tRNA^{Phe}	164 ± 5	0.184 ± 0.040	39 ± 5
RP-WT-tRNA^{Phe}-MRP	137 ± 13	0.147 ± 0.032	41 ± 2
tRK1-WT-tRNA^{Phe}	134 ± 9	0.153 ± 0.049	41 ± 4
tRNA^{Phe} (yeast)	168 ± 12	0.148 ± 0.047	39 ± 3

Data represent the mean ± SD (n = 3–8).

designed to have two mismatches at the 3′ terminal side, and a point mutation (G625A in mtDNA) was detected (Figure 4B). For example, the WT primer can detect a wild-type gene because the C in the 3′ terminal of the WT primer can bind 625G in a wild-type gene to elongate, whereas the WT primer cannot bind to 625A in the mutant gene, and therefore, the mutant gene cannot be detected (Figure 4Ba). The primers used in this evaluation are summarized in Table 2. In this study, pDNA encoding the target wild-type gene and the mutant gene (pT7-WT-tRNA^{Phe} and pT7-MT-tRNA^{Phe}) were mixed at a ratio of 0% to 100%, and quantitative ARMS-PCR was performed in each solution using a WT primer and a MT primer. The mutation rate was calculated using Equation 1, shown in Materials and Methods, and the tRNA^{Phe} mutation rate was determined using the prepared calibration curve.

To validate this evaluation method, the mutation rate of mitochondrial RNA in G625A fibroblasts was measured by the above method, and it was found that the mutation rate was about 80%. This value was in agreement with the 80% reported as mtDNA mutation rate in a previous study.[5] Because G625A cells are primary cultured cells obtained from skin biopsies of patients, we concluded that it might be possible that the mutation rate could change by continuing passaging. Therefore, the mutation rate from the start of cell culture to the 23rd day was determined (Table S1). No change in the mutation rate was observed from day 13 to day 23 after the start of the culture. In addition, the mutation rates of mitochondrial RNA in HeLa cells and normal fibroblasts (NB1RGB cells), which do not contain mutated tRNA^{Phe}, were determined to be about 0%. These results indicate that the constructed mutation rate detection method is valid and can be used.

Evaluation of the Mutation Rate of tRNA^{Phe} in Mitochondria of G625A Patient Cells after the Transfection of Therapeutic tRNA

We investigated the issue of whether the mutation rate of tRNA^{Phe} in mitochondria of G625A cells was decreased when the direct mitochondrial transfection of therapeutic RNA was performed using the MITO-Porter system. MITO-Porter (pre-WT-tRNA^{Phe}), MITO-Porter (RP-WT-tRNA^{Phe}-MRP), MITO-Porter (tRK1-WT-tRNA^{Phe}), or MITO-Porter (tRNA^{Phe} (yeast)) were added to G625A cells, and the mutation rate of tRNA^{Phe} was estimated using the ARMS-PCR method (Figure 5A). As a result, the mutation rates of tRNA^{Phe} were dramatically decreased at day 2 and day 4 after the mitochondrial transfection of pre-WT-tRNA^{Phe}, RP-WT-tRNA^{Phe}-MRP, and tRK1-WT-tRNA^{Phe}, whereas the value was not decreased in the case of tRNA^{Phe} (yeast), the negative control. This therapeutic effect was sustained even on the 8th day after transfection (Table S2). In addition, the mutation rate of tRNA^{Phe} was reduced to about 20% at an early stage (2 days) after the mitochondrial transfection of tRK1-WT-tRNA^{Phe}. In normal fibroblasts (NB1RGB cells), the mutation rate of tRNA^{Phe} remained essentially constant after the mitochondrial transfection of pre-WT-tRNA^{Phe} (data not shown).

We also evaluated heteroplasmy levels of tRNA^{Phe} in mitochondria after the mitochondrial delivery of the tRNA via the allotropic expression system. For allotropic expression, we transfected pDNA with a CMV promoter to produce nuclear-expressed tRNA^{Phe} (pCMV-WT-tRNA^{Phe}, pCMV-RP-WT-tRNA^{Phe}-MRP, pCMV-tRK1-WT-tRNA^{Phe}, and pCMV-WT-tRNA^{Phe} (yeast)) using Lipofectamine 2000 (LFN 2000) (Figure 5B). Since RP-WT-tRNA^{Phe}-MRP and tRK1-WT-tRNA^{Phe} contain a mitochondrial import sequence, it was expected that the transfection of these pDNAs into the nucleus would result in the mitochondrial delivery of nuclear-expressed tRNA^{Phe}. However, the mutation rate of tRNA^{Phe} did not decrease to less than the value when pCMV-WT-tRNA^{Phe} (yeast), negative control, was transfected.

Investigation of the Influence of a Decrease in the Mutation Rate of tRNA^{Phe} on Mitochondrial Function

We investigated the influence of a decrease in the rate of mutation when therapeutic tRNA was delivered to mitochondria on the mitochondrial respiratory capacity. The mitochondrial transfection of pre-WT-tRNA^{Phe} (therapeutic tRNA) or tRNA^{Phe} (yeast) (negative control) into G625A cells by the MITO-Porter system and mitochondrial respiratory capacity was measured using Oxygraph-2k[24] at 3 days after the transfection. As a result, mitochondrial respiratory capacity of the G625A cells was increased after the transfection of therapeutic pre-WT-tRNA^{Phe} to mitochondria compared to the tRNA^{Phe} (yeast) (Figure 6A). On the other hand, it was observed that mitochondrial respiratory capacity remained essentially unchanged in NB1RGB cells (normal cells) (Figure 6B).

We also carried out a long-term evaluation of mitochondrial respiratory activity (Figure S1). We transfected therapeutic RNA into diseased cells and evaluated the mitochondrial respiratory activities after 3, 8, and 10 days after the transfection. As a result of the evaluation, the therapeutic effect was sustained even on the 10th day. This was the same tendency for which the decrease in mutation rate was retained, as shown in Table S2.

We also evaluated ATP production levels in tRNA-transfected cells. In the case of G625A cells, the mitochondrial transfection of therapeutic tRNA, including pre-WT-tRNA^{Phe} and tRK1-WT-tRNA^{Phe} by the MITO-Porter system, resulted in a significant increase in ATP production levels compared to that of tRNA^{Phe} (yeast) (Figure 7A). The mitochondrial transfection of therapeutic tRNA had no effect on ATP production levels in the case of NB1RGB cells (normal cells) (Figure 7B). We also confirmed that mitochondrial

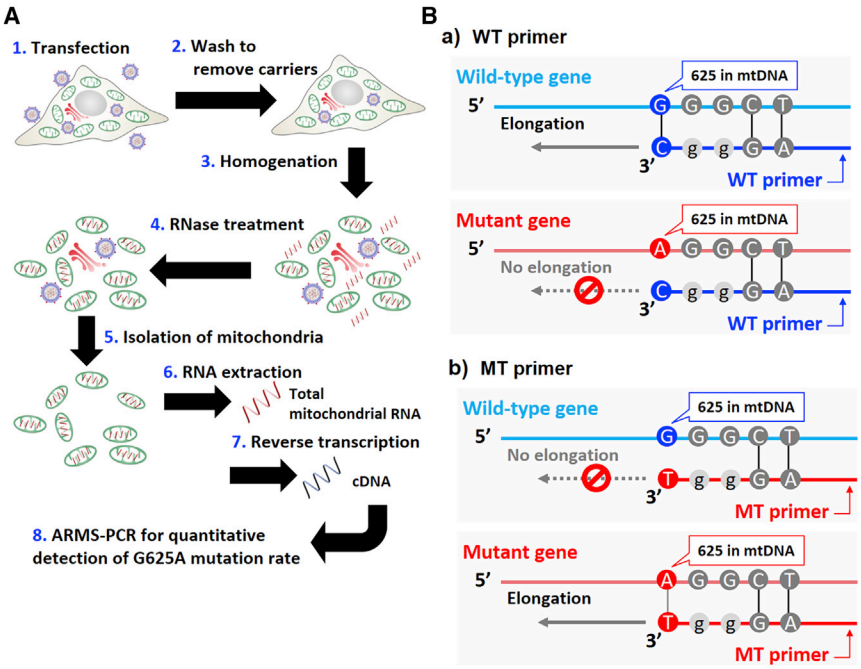

Figure 4. Schematic Protocol for Evaluating the Mutation Rate of tRNA^{Phe} in Mitochondria after Transfection

(A) Scheme showing the mutation rate of tRNA^{Phe} extracted from mitochondria of disease cells. Transfection of therapeutic RNA into diseased cells with the MITO-Porter (step 1), and the cells are then washed in order to remove MITO-Porter bound to the surface of cell membranes (step 2). Cells are homogenized using a syringe needle, and fraction containing nuclei and fracted cells are removed by centrifugation (step 3). The resulting fraction is treated with RNase to remove tRNA^{Phe} outside the mitochondria (step 4), and mitochondria are isolated by density gradient centrifugation (step 5). Finally, total RNAs are extracted from the isolated mitochondria (step 6), cDNAs are prepared using reverse transcription reaction (step 7), and ARMS-PCR is then used for the quantitative determination of G625A mutation rate (step 8). (B) Design of reverse primers to distinguish G and A at 625 in mtDNA coding tRNA^{Phe} using ARMS-PCR. In this experiment, reverse primers were designed to have two mismatches at the 3′ terminal side. The WT primer can detect the wild-type gene because the C localized at the 3′ terminal of the WT primer can bind 625G in the wild-type gene to elongate it, whereas the WT primer cannot bind to 625A in the mutant gene, which makes the mutant gene undetectable (a). In similar way, the MT primer can detect only 625A in the mutant gene (b). Primers used in this evaluation are summarized in Table 2.

transfection using the MITO-Porter had no effect on cell viability in both types of cells (Figure S2). These results indicate that mitochondrial function would be increased by delivering therapeutic tRNA to G625A cells using the MITO-Porter.

DISCUSSION

Although mRNA and rRNA, derived from nuclear DNA, are not transported to mitochondria, some tRNA has been detected in mitochondria,[25] which indicates the possibility that tRNA in the cytoplasm is actually transported to mitochondria. The pathway for the transport of tRNA to mitochondria has not been identified, but association of translocase of mitochondrial outer membrane (TOM)/translocase of mitochondrial outer membrane (TIM) complex, voltage-dependent anion channel (VDAC), mitochondrial polynucleotide phosphorylase (PNPase), etc., has been reported.[9,26] Since small molecules easily pass through the mitochondrial outer membrane, the possibility that tRNAs themselves might be transported to the matrix through a mitochondrial transporter cannot be excluded. Therefore, a portion of the tRNA in the cytoplasm may be transported into mitochondria, even if mitochondrial delivery by the MITO-Porter was not achieved.

In this study, the RP sequence, as shown in the Supplemental Information, was used, because this sequence has frequently been reported to serve as a mitochondrial import sequence for RNA.[8] It has been reported that the 3′ UTR sequences of mRNA coding the mitochondrial ribosomal protein S12 (MRPS12), superoxide dismutase 2 (SOD2), and mitochondrial ATP synthetase, beta subunit (ATP5B), bind to certain proteins, resulting in their being imported to ribosomes that are localized in mitochondrial membranes.[27] Wang et al.[17] reported that the addition of these 3′ UTR sequences to target RNA molecules increased mitochondrial transport. Based on previous reports, we designed RP-WT-tRNA^{Phe}-MRP that contains RP at the 5′ end and MRP, which is capable of binding to the mitochondrial membrane, at the 3′ end. We also evaluated tRK1-WT-tRNA^{Phe} containing a tRK1 sequence derived from yeast tRNA Lys (CTT) with mitochondrial import activity.[6]

As shown in Figure 5A, when pre-WT-tRNA^{Phe}, RP-WT-tRNA^{Phe}-MRP, and tRK1-WT-tRNA^{Phe} were transfected with the MITO-Porter, the tRNA^{Phe} mutation rate was decreased the most in the case of the mitochondrial transfection of tRK1-WT-tRNA^{Phe}. As mentioned above, some tRNA in the cytoplasm might be delivered to mitochondria, but it has been reported that the tRK1 sequence is transported to human mitochondria. Thus, it appears that tRK1-WT-tRNA^{Phe} was easily delivered to mitochondria of human cells. In the case of the use of the MITO-Porter system, the tRK1-WT-tRNA^{Phe} that remained in the cytosol had leaked from the MITO-Porter and in the intermembrane space after fusion with the mitochondrial outer membrane, would be imported into the mitochondrial matrix via the tRK1 sequence.

As shown in Figure 5B, when tRNA^{Phe} is delivered to mitochondria via allotropic expression, the mutation rates were comparable among

Table 2. Primers Used for ARMS-PCR to Detect G625A Point Mutation

Primers	Nucleotide Sequence (5′–3′)	Note
Common primer (+)	GCTTACCTCCTCAAAGCAATACACTG	common forward primer binding to the sequence of the $tRNA^{Phe}$ gene in mtDNA corresponding to 586–611 bases
WT primer (−)	GTTTATGGGGTGATGTGAGgg**C**	reverse primer for elongation by recognizing 625**G** (wild type) in the sequence of the $tRNA^{Phe}$ gene in mtDNA
MT primer (−)	GTTTATGGGGTGATGTGAGgg**T**	reverse primer for elongation by recognizing 625**A** (mutant) in the sequence of the $tRNA^{Phe}$ gene in mtDNA

Reverse primer binding to the sequence of the $tRNA^{Phe}$ gene in mtDNA corresponding to 625–646 bases. Lowercase letters indicate mismatches.

RNAs with and without mitochondrial import sequences, such as an RP sequence, suggesting that mitochondrial import sequences might not work under such conditions. It has been reported that the RP sequence requires certain proteins that are included in cytoplasmic extracts and ATP for mitochondrial delivery in experiments using isolated mitochondria. Moreover, Wang et al.[17] reported that only a limited number of RNA molecules are transported to mitochondria by mitochondrial import sequences via the allotropic expression system. Based on previous reports, differences in mitochondrial delivery in the presence and absence of mitochondrial import sequences in this study would be hardly observed.

We also verified the mitochondrial delivery of pre-WT-$tRNA^{Phe}$ (mutant tRNA) by these sequences via allotopic expression in normal cells (NB1RGB cells). As a result, in normal cells, a mutation rate of about 15% was confirmed, although the efficiency was very low (data not shown). With the consideration of these results, the absence of mitochondrial delivery in the diseased cells by allotopic expression might have been caused by mitochondrial dysfunction in disease cells. When the direct mitochondrial transfection of the RNA was carried out using the MITO-Porter, the RNA with the mitochondrial targeting signal sequences was found to reduce the mutation rate more efficiently than RNA that was devoid of the sequences. This result indicates that the RNA, which was delivered in close proximity to mitochondria, might have been efficiently transported to the interior of mitochondria by the mitochondrial targeting signal sequences.

Mitochondrial genetic diseases lead to dysfunction in multiple organs, and brain damage is particularly serious. However, the delivery of nucleic acids to the brain through the blood brain barrier is a formidable hurdle. On the other hand, it would be expected that the local administration of a MITO-Porter in tissues, such as muscles, eyes, and ears, in which this disease is involved, could be realized in the near future. In this study, although we validated a mitochondrial gene therapeutic strategy using therapeutic RNA, we conclude that a similar strategy could be achieved in the case of the mitochondrial delivery of therapeutic DNA and proteins.

In conclusion, MITO-Porters encapsulating WT-$tRNA^{Phe}$ and analogs with mitochondrial import sequences as therapeutic RNAs could be delivered to mitochondria of fibroblasts in patients with a mitochondrial disease (G625A fibroblast), resulting in a decrease in the mutation rate of $tRNA^{Phe}$ in mitochondria. Moreover, a decrease in the mutation rate would improve mitochondrial function in the G625A fibroblast. This study represents the world's first report of mitochondrial tRNA delivery using a nano capsule to show therapeutic function in mitochondrial disease cells. Based on these results, we conclude that a MITO-Porter system promises to be a potentially useful mitochondrial drug delivery system (DDS) for achieving mitochondrial gene therapy.

MATERIALS AND METHODS

The experiment protocol using G625A fibroblasts from a mitochondrial disease patient was approved by the ethics boards of the Faculty of Pharmaceutical Sciences, Hokkaido University (number 2014-003 from 10/17/2014), Hokkaido University Hospital (number 14-061 from 1/1/2015), and Sapporo City General Hospital (number H26-050-224 from 1/14/2015) and performed under ethical guidelines on human genome and materials. Written, informed consent was obtained from parents of the patient.

Materials

1,2-dioleoyl-sn-glycero-3-phosphatidyl ethanolamine (DOPE), DOPE-*N*-(7-nitro-2-1,3-benzoxadiazole-4-yl) (NBD-DOPE), and sphingomyelin (SM) were purchased from Avanti Polar Lipids (Alabaster, AL, USA). Stearylated R8 (STR-R8)[28] was obtained from Kurabo Industries (Osaka, Japan). Protamine was purchased from Calbiochem (Darmstadt, Germany). pTriEx3 Neo vector was purchased from Merck (Novagen; Darmstadt, Germany). LFN 2000 was purchased from Life Technologies (Carlsbad, CA, USA). Fetal bovine serum (FBS), MitoTracker Deep Red, and Rhodamine 123 were purchased from Thermo Fisher Scientific Life Sciences (Waltham, MA, USA). Dulbecco's modified Eagle's medium (DMEM) with high glucose and minimum essential medium Eagle alpha modification (α-MEM) were purchased from Nacalai Tescue (Kyoto, Japan). Oligonucleotides, in purified form, were purchased from Sigma Genosys Japan (Ishikari, Japan). All other chemicals used were commercially available reagent-grade products.

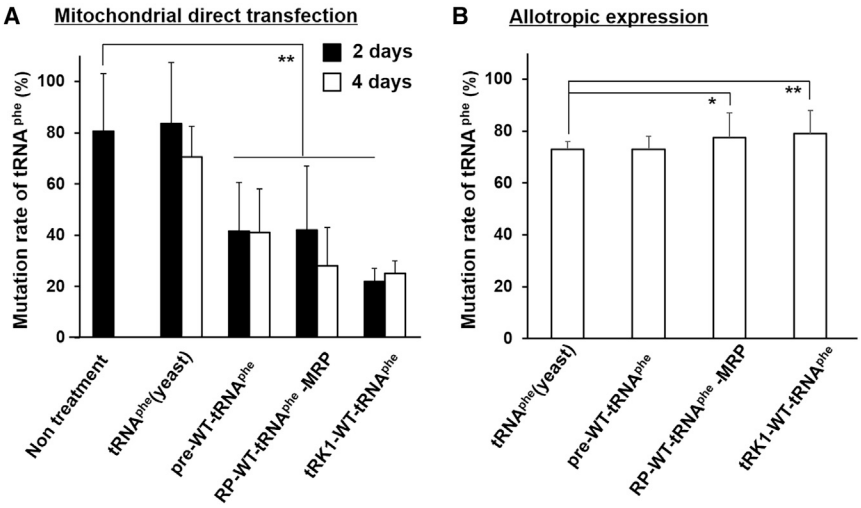

Figure 5. Evaluation of the Mutation Rate of tRNA^{Phe} in Mitochondria of G625A Cells after Transfection

(A) Evaluation of the mutation rate of tRNA^{Phe} after direct mitochondrial transfection. G625A fibroblasts were transfected with RNA (tRNA^{Phe} (yeast), pre-WT-tRNA^{Phe}, RP-WT-tRNA^{Phe}-MRP, and tRK1-WT-tRNA^{Phe}) using the MITO-Porter system. Mutation rates were measured at 2 days (closed bars) and 4 days (open bars) after the transfection. Bars represent the mean ± SE (n = 3–4). Significant differences (versus nontreatment) were calculated by one-way ANOVA, followed by the Bonferroni test (**$p < 0.01$). (B) Evaluation of the mutation rate of tRNA^{Phe} after mitochondrial RNA delivery via allotropic expression. G625A fibroblasts were transfected with several kinds of pDNAs coding tRNA by Lipofectamine 2000, and the mutation rates were measured at 4 days after the transfection. Bars represent the mean ± SE (n = 3). Significant differences (versus tRNA^{Phe} (yeast)) were calculated by one-way ANOVA, followed by the Bonferroni test (**$p < 0.01$, *$p < 0.05$).

Cell Culture

G625A fibroblasts were obtained from a mitochondrial disease patient at the Sapporo City General Hospital. The G625A fibroblasts carry a heteroplasmic mutation in the tRNA for phenylalanine in the mitochondrial DNA, leading to a decreased complex III activity. The phenotype includes epilepsy, hearing loss, and elevated lactate levels.[5] The normal human skin fibroblasts, NB1RGB (RCB0222), were provided by the Riken BioResource Research Center (BRC) through the National Bio-Resource Project of the Ministry of Education, Culture, Sports, Science and Technology (MEXT)/Japan Agency for Medical Research and Development (AMED), Japan. The G625A fibroblasts and NB1RGB were maintained in DMEM with high glucose and α-MEM, respectively. The mediums contained 10% FBS, supplemented with penicillin and streptomycin. Cells were grown in 10 cm dishes at 37°C under 5% CO_2 until reaching approximately 80% confluence. Cell passage was performed every 2–4 days.

Construction and Preparation of pDNA Containing the Therapeutic tRNA Gene

The gene fragments for pT7-WT-tRNA^{Phe}, pT7-RP-WT-tRNA^{Phe}-MRP, pT7-tRK1-WT-tRNA^{Phe}, and pT7-tRNA^{Phe} (yeast) were synthesized by Genewiz (South Plainfield, NJ, USA), and the synthesized genes were inserted into the pUC57-Amp vector (Genewiz) that had been pretreated with the restriction enzymes (EcoRI and BglII sites) (Figure 2Ba–d). For the construction of pT7-MT-tRNA^{Phe}, a point mutation (G → A) was inserted in pT7-MT-tRNA^{Phe} by the PrimeSTAR Mutagenesis Basal Kit (Takara Bio, Shiga, Japan) using the following pair of primers: 5′-tttagac**A**ggctcacatcaccccataa-3′ (forward) and 5′-gtgagcc**T**gtctaaacattttcagtgt-3′ (reverse), according to the manufacturer's recommended protocol. Sequences in bold uppercase letters initiate mutation point (G625A) in pT7-WT-tRNA^{Phe}. To construct the pDNA vector with CMV for allotropic expression, the DNA fragments derived from pT7-WT-tRNA^{Phe}, pT7-RP-WT-tRNA^{Phe}-MRP, pT7-tRK1-WT-tRNA^{Phe}, and pT7-tRNA^{Phe} (yeast) were pretreated with the restriction enzymes (EcoRI and BglII sites), and the DNA fragments (EcoRI and BglII fragment) were inserted into the pTriEx3 Neo vector with the CMV promoter pretreated with the same restriction enzymes to construct pCMV-WT-tRNA^{Phe}, pCMV-RP-WT-tRNA^{Phe}-MRP, pCMV-tRK1-WT-tRNA^{Phe}, and pCMV-tRNA^{Phe} (yeast) (Figure 2Be). The sequence information of these plasmids is summarized in Vector Sequences S1–S5. The pDNA used in this experiment was amplified in *E. coli* strain DH5α, purified using an Endofree Plasmid Midi Kit (QIAGEN, Hilden, Germany).

Purification of RNA via an *In Vitro* Transcription System

RNAs (WT-tRNA^{Phe}, WT-tRNA^{Phe}-MRP, tRK1-WT-tRNA^{Phe}, and tRNA^{Phe} (yeast)) were purified using pT7-WT-tRNA^{Phe}, pT7-RP-WT-tRNA^{Phe}-MRP, pT7-tRK1-WT-tRNA^{Phe}, and pT7-tRNA^{Phe} (yeast) as template pDNAs via the *in vitro* transcription system, including the T7 RNA polymerase, as described below. Linear DNAs were prepared by digestion of the pDNA with EcoRV, the linear DNAs, and then purified by phenol/chloroform extraction and ethanol precipitation. *In vitro* transcription was performed to synthesize RNAs using the linear DNAs as templates, according to the manufacturer's recommended protocol of the RiboMAX Large Scale RNA Production System (Promega, Madison, WI, USA). An appropriate amount of DNase I was added and incubated at 37°C for 15 min. The synthesized RNAs were purified, according to the manufacturer's recommended protocol of NucleoSpin RNA Clean-up (Machery-Nagel, Duren, Germany). The concentrations and purities of the purified RNA were measured using a NanoDrop (ND-2000; Thermo Fisher Scientific).

Packaging Therapeutic tRNA in MITO-Porter

MITO-Porter encapsulating nanoparticles of tRNA were constructed by the ethanol dilution method. A solution of tRNA (pre-WT-tRNA^{Phe}, WT-tRNA^{Phe}-MRP, tRK1-WT-tRNA^{Phe}, or tRNA^{Phe} (yeast)) in 10 mM HEPES buffer (pH 7.4) was mixed with a protamine solution to form a tRNA nanoparticle at an N/P ratio of 0.9. The MITO-Porter

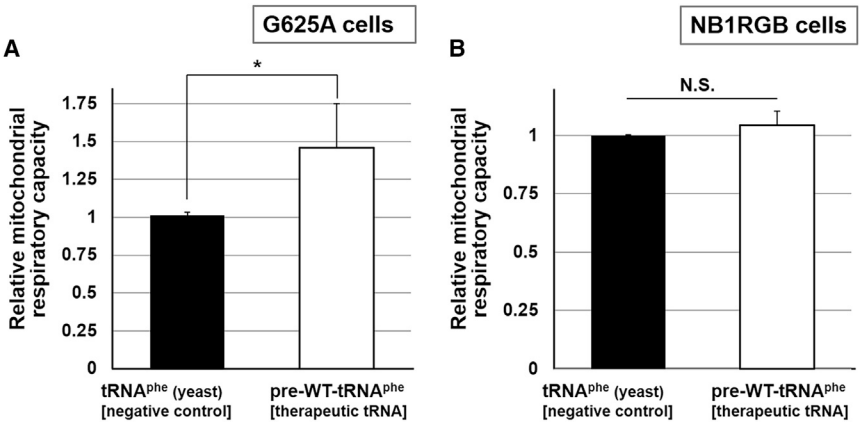

Figure 6. Evaluation of Mitochondrial Respiratory Capacity in Pre-WT-tRNA^{Phe}-Transfected Cells

Mitochondrial respiratory capacities of G625A cells (A) or NB1RGB cells (normal cells) (B) were measured by Oxygraph-2k at 72 h after the mitochondrial transfection of pre-WT-tRNA^{Phe} (therapeutic tRNA) or tRNA^{Phe} (yeast) (negative control) by the MITO-Porter system. Relative mitochondrial respiratory capacities were normalized with the value of tRNA^{Phe} (yeast)-transfected cells as 1. Data are represented as the mean ± SE (n = 3–5). *$p < 0.05$, significant difference analyzed by Student's t test. N.S., no significant difference by Student's t test.

had a component molar ratio of DOPE/SM/STR-R8 (molar ratio: 9/2/1). A 115-μL portion of a 100% (v/v) EtOH solution of the lipids (240 nmol) was titrated slowly with 65 μL of tRNA nanoparticle (9.75 μg of tRNA) under vigorous mixing to avoid a low local concentration of EtOH and diluted quickly with HEPES buffer to a final concentration of <20% EtOH. The ethanol was removed by ultrafiltration using Amicon Ultra-5-100K (Merck; Merck Millipore), with the external buffer replaced by HEPES buffer and the solution then concentrated to give the MITO-Porter encapsulating tRNA.

Particle diameters and PDI as an indicator of particle-size distribution were measured using a dynamic light scattering (DLS) method (Zetasizer Nano ZS; Malvern Instruments, Worcestershire, UK). Samples were prepared in 10 mM HEPES buffer at 25°C, and the values for particle diameters are shown in the form of volume distribution. The ξ-potentials of the samples were also determined in 10 mM HEPES buffer at 25°C using a Zetasizer Nano ZS.

Intracellular Observation of the MITO-Porter by CLSM

Empty MITO-Porters containing 0.5 mol% NBD-DOPE (green fluorescent lipid) were prepared by the lipid hydration method, as previously reported.[10,29] Cells were seeded in 35 mm glass-bottom dishes (AGC Techno Glass [IWAKI], Shizuoka, Japan), 24 h prior to the experiment (2 mL, 8×10^4 cells/mL, incubation at 37°C, 5% CO_2). After washing the cells twice with 1 mL DMEM (FBS−), they were incubated with DMEM that did not contain FBS and in the presence of the MITO-Porter (10 nM lipid) for 1 h. The medium was removed, and 1 mL of DMEM (FBS+) was added. After incubation for a further 1 h and 40 min, the cells were stained with MitoTracker Deep Red (1 mL, final concentration 100 nM), 20 min prior to observation. Cells were washed with DMEM (phenol red−), and 1 mL of fresh DMEM (phenol red−) was added before CLSM images were obtained using a FV10i-LIV (Olympus, Tokyo, Japan). The cells were excited with a 473-nm light and a 635-nm light from an laser Diode (LD) laser. Images were obtained using an FV10i-LIV equipped with a water-immersion objective lens (UPlanSApo 60×/numerical aperture [NA] 1.2) and a dichroic mirror (DM405/473/559/635). The two fluorescence detection channels (Ch) were set to the following filters: Ch1: 490/50 (green) for NBD-DOPE; Ch2: 660/50 (red) for MitoTracker Deep Red.

Transfection of Therapeutic RNA for Quantification of the Mutation Rate of tRNA^{Phe} by ARMS-PCR

Cells were seeded on 6-well plates (Becton Dickinson [Corning], Franklin Lakes, NJ, USA), 24 h prior to the experiment (2 mL, 1×10^5 cells/mL, incubation at 37°C, 5% CO_2). After washing the cells with 1 mL of phosphate-buffered saline (PBS (−)), the cells were incubated with medium that did not contain FBS and in the presence of the MITO-Porter (pre-WT-tRNA^{Phe}) (6.75 nM RNA [300 ng RNA]) for 3 h for direct mitochondrial transfection. MITO-Porter (RP-WT-tRNA^{Phe}-MRP), MITO-Porter (tRK1-WT-tRNA^{Phe}), or MITO-Porter (tRNA^{Phe} (yeast)) were also added to the cells at similar way (6.75 nM RNA). For allotropic expression, pCMV-WT-tRNA^{Phe}, pCMV-RP-WT-tRNA^{Phe}-MRP, pCMV-tRK1-WT-tRNA^{Phe}, or pCMV-WT-tRNA^{Phe} (yeast) were transfected to cells using LFN 2000, according to the manufacturer's recommended protocol (1 μg). After the incubation, the medium was replaced with complete medium containing FBS and further incubated at 37°C, 5% CO_2, for 45 h or 93 h. After washing the cells with 1 mL PBS (−), they were treated with 500 μL of PBS (−) containing trypsin to remove cells. After incubation of the cells at 37°C, 5% CO_2, for 3 min, 1 mL of complete medium was added to the cells, followed by centrifugation at 700 × *g* at 4°C for 3 min. The supernatant was removed to obtain the collected cells (step 2).

Quantification of the Mutation Rate of tRNA^{Phe} in Mitochondria by ARMS-PCR

A schematic protocol is shown in Figure 4A. The cells collected, as mentioned above, were suspended in 100 μL of CellScrub buffer (Genlantis, San Diego, CA, USA) to remove carriers bound to the surface of cell membranes (step 2). After shaking at 4°C for 15 min, the cell suspension was centrifuged at 700 × *g* for 3 min at 4°C, and the pelleted fraction was resuspended in 500 μL of mitochondrial isolation buffer (MIB; 250 mM sucrose, 2 mM Tris-HCl, 1 mM EDTA, pH 7.4). The resulting suspension was homogenized with a 27-gauge needle (step 3) and centrifuged at 700 × *g* for 10 min at 4°C to remove

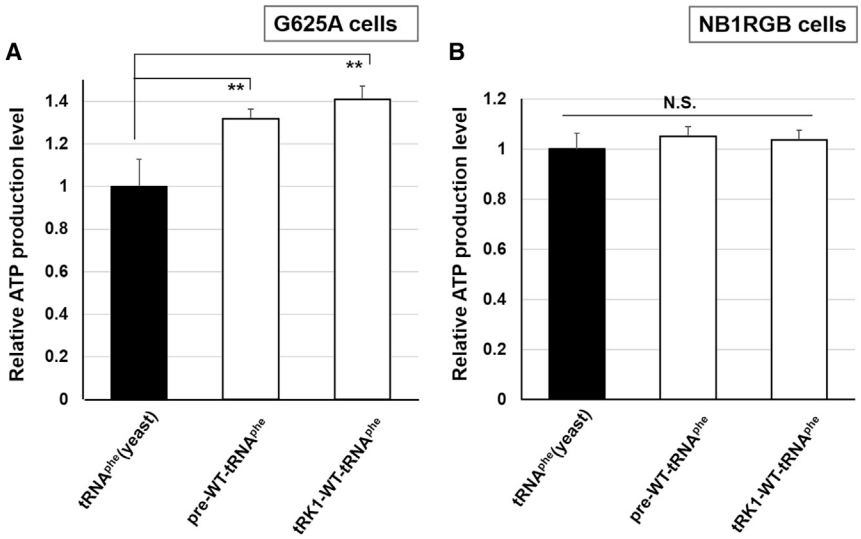

Figure 7. Evaluation of the Levels of ATP Production in Pre-WT-tRNA^{Phe}-Transfected Cells

Levels of ATP production in G625A cells (A) or NB1RGB cells (normal cells) (B) were measured by Mitochondrial ToxGlo Assay at 96 h after mitochondrial transfection of pre-WT-tRNA^{Phe}, tRK1-WT-tRNA^{Phe}, or tRNA^{Phe} (yeast) (negative control) by the MITO-Porter system. Relative ATP production levels were normalized with the value for the tRNA^{Phe} (yeast)-transfected cells as 1. Data are represented as the mean ± SE (n = 4–8). **p < 0.01, significant differences (versus tRNA^{Phe} (yeast)) were calculated by one-way ANOVA, followed by the Bonferroni test. N.S., no significant difference by one-way ANOVA.

the fraction containing nuclei and fracted cells. The resulting supernatant containing mitochondria was treated with RNase to remove RNA outside the mitochondria (step 4) and centrifuged at 700 × *g* for 10 min at 4°C. The resulting supernatant was added onto a 60% Percoll solution (GE Healthcare UK, Buckinghamshire, UK) and centrifuged at 20,400 × *g* for 10 min at 4°C. The mitochondria present on the interface between the Percoll solution and MIB was collected and centrifuged at 16,000 × *g* for 15 min at 4°C. After removal of the supernatant, the pelleted fraction was resuspended in 500 μL of EDTA-free MIB (250 mM sucrose, 2 mM Tris-HCl, pH 7.4) and centrifuged at 16,000 × *g* for 15 min at 4°C. The supernatant was removed to obtain a mitochondrial fraction (step 5). Total RNAs were extracted from the isolated mitochondria (step 6) with an RNeasy Mini Kit (QIAGEN, Hilden, Germany), according to the manufacturer's protocol, combined with DNase I digestion for the degradation of DNA in total RNA samples using the RNase-Free DNase Set (QIAGEN). The resulting RNA suspension was reverse transcribed (step 7) using a High-Capacity RNA-to-cDNA Kit (Thermo Fisher Scientific [Applied Biosystems]), according to the manufacturer's protocol. In this kit, cDNA is synthesized from various RNA species using "random primers," enabling DNA synthesis from RNA without a poly A sequence. Thus, we were able to synthesize mitochondrial total RNA containing tRNA.

A quantitative ARMS-PCR analysis was performed on the cDNA using the THUNDERBIRD SYBR qPCR Mix (Toyobo, Osaka, Japan) and LightCycler 480 (Sigma-Aldrich [Roche]). All reactions were performed using a volume of 5 μL. In this experiment, a common forward primer (common primer (+)) binding to the sequence of the tRNA^{Phe} gene in the mtDNA corresponding to 586–611 bases was used, and the reverse WT primer (−) for recognition of 625G in the sequence of the tRNA^{Phe} gene in the mtDNA (wild type) and reverse MT primer (−) for recognition of 625A in the sequence of the tRNA^{Phe} gene in the mtDNA (mutant) were designed. Reverse primers binding to the sequence of the tRNA^{Phe} gene in the mtDNA are corresponding to 625–646 bases. The sequences of primers used for the real-time PCR are shown in Table 2. In this study, pDNA encoding the target wild-type gene and mutant gene (pT7-WT-tRNA^{Phe} and pT7-MT-tRNA^{Phe}) was mixed at a ratio of 0% to 100% for a standard curve, and quantitative ARMS-PCR was performed in each solution using a common forward primer and two kinds of reverse primers. Briefly, we estimated the difference in threshold cycles (ΔC_T) between the wild-type gene and the mutant gene: $\Delta C_T = (\Delta C_{T\text{wild-type}} - \Delta C_{T\text{mutant}})$ using each set of samples. Each reaction was done, at least in duplicate. The mutation rate was calculated using Equation 1, as described below:

$$\text{Mutation rate of tRNA}^{Phe}(\%) = \frac{1}{1+\left(\frac{1}{2}\right)^{\Delta C_T}} \times 100. \quad \text{(Equation 1)}$$

Evaluation of Mitochondrial Respiratory Capacity

Cells were seeded on a 10-cm cell-culture dish (Thermo Fisher Scientific (Falcon), Waltham, MA., USA) at 24 ± 3 h prior to the experiment (10 mL, 1 × 10^5 cells/mL, incubation at 37°C, 5% CO_2). After washing the cells with 5 mL PBS (−), they were incubated with medium that did not contain FBS and in the presence of the MITO-Porter (pre-WT-tRNA^{Phe}) or MITO-Porter (tRNA^{Phe} (yeast)) (6.75 nM RNA) for 3 h for direct mitochondrial transfection. After the incubation, the medium was replaced with complete medium containing FBS and further incubated at 37°C, 5% CO_2, for 69 h. After washing the cells with 5 mL PBS (−), the cells were incubated with 2 mL of PBS (−) containing trypsin to remove cells. After incubation of the cells at 37°C, 5% CO_2, for 5 min, 8 mL of complete medium was added to the cells, followed by centrifugation at 700 × *g* for 5 min at 4°C. After removal of the supernatant, the pelleted fraction was resuspended in 10 mL of PBS (−) and centrifuged at 700 × *g* for 5 min at 4°C. After removal of the supernatant, the pelleted fraction was resuspended in 500 μL of mitochondrial respiration medium-MiR05 (110 mM sucrose, 60 mM potassium lactobionate, 0.5 mM ethylene glycol tetraacetic acid, 3 mM $MgCl_2$, 20 mM taurine, 10 mM KH_2PO_4, 20 mM HEPES, pH 7.1, and 1% BSA). Mitochondrial respiratory capacity measurements were then performed using high-resolution respirometry Oroboros Oxygraph-2k (Oroboros Instruments,

Innsbruck, Austria). The Oxygraph-2k detects changes in O_2 concentration of the cells with an oxygen sensor when various substrates and inhibitors are sequentially added to 5 μM digitonin-permeabilized cells. In this experiment, the mitochondrial respiratory capacity is indicated by the detection of oxidative phosphorylation upon the addition of 2 mM malate (Mal), 10 mM glutamate (Glu), 5 mM pyruvate (Pyr), 3 mM $MgCl_2$, and 10 mM ADP, as previously described.[30,31] Relative mitochondrial respiratory capacities were normalized with the value of $tRNA^{Phe}$ (yeast)-transfected cells as 1.

Evaluation of ATP Production and Cell Viability

Cells (1×10^4 cells/well) were incubated in a 96-well plate (Becton Dickinson [Corning]) with medium containing 10% FBS under an atmosphere of 5% CO_2/air at 37°C for 24 ± 3 h. After washing the cells with 100 μL PBS (−), they were incubated with medium that did not contain FBS and in the presence of samples for 3 h (37°C, 5% CO_2). After the incubation, the medium was replaced with complete medium containing serum, followed by a further incubation for 93 h. The amounts of ATP production and cell viability were measured using a Mitochondrial ToxGlo Assay (Promega) by an EnSpire 2300 Multilabel Reader (PerkinElmer, Waltham, MA, USA). Relative ATP production levels and relative cell viabilities were normalized with the value of $tRNA^{Phe}$ (yeast)-transfected cells as 1, respectively.

Statistical Analysis

For comparisons of the two groups, the statistical significance was calculated by the Student's t test. For multiple comparisons, one-way ANOVA was performed, followed by the Bonferroni/Dunn test. Levels of $p < 0.05$ were considered to be significant.

SUPPLEMENTAL INFORMATION

Supplemental Information can be found online at https://doi.org/10.1016/j.omtn.2020.04.004.

AUTHOR CONTRIBUTIONS

The manuscript was written through contributions of all authors. All authors have given approval to the final version of the manuscript.

CONFLICTS OF INTEREST

The authors declare no competing interests.

ACKNOWLEDGMENTS

We thank Dr. Milton Feather for his helpful advice in writing the manuscript. This work was supported by Grants-in-Aid for Scientific Research (B) (26282131 and 17H02094 to Y.Y.) from the Ministry of Education, Culture, Sports, Science and Technology and Japanese Government (MEXT).

REFERENCES

1. Schwerzmann, K., Cruz-Orive, L.M., Eggman, R., Sänger, A., and Weibel, E.R. (1986). Molecular architecture of the inner membrane of mitochondria from rat liver: a combined biochemical and stereological study. J. Cell Biol. *102*, 97–103.
2. Legros, F., Malka, F., Frachon, P., Lombès, A., and Rojo, M. (2004). Organization and dynamics of human mitochondrial DNA. J. Cell Sci. *117*, 2653–2662.
3. Stewart, J.B., and Chinnery, P.F. (2015). The dynamics of mitochondrial DNA heteroplasmy: implications for human health and disease. Nat. Rev. Genet. *16*, 530–542.
4. Schapira, A.H. (2012). Mitochondrial diseases. Lancet *379*, 1825–1834.
5. Sudo, A., Takeichi, N., Hosoki, K., and Saitoh, S. (2011). Successful cochlear implantation in a patient with mitochondrial hearing loss and m.625G>A transition. J. Laryngol. Otol. *125*, 1282–1285.
6. Karicheva, O.Z., Kolesnikova, O.A., Schirtz, T., Vysokikh, M.Y., Mager-Heckel, A.M., Lombès, A., Boucheham, A., Krasheninnikov, I.A., Martin, R.P., Entelis, N., and Tarassov, I. (2011). Correction of the consequences of mitochondrial 3243A>G mutation in the MT-TL1 gene causing the MELAS syndrome by tRNA import into mitochondria. Nucleic Acids Res. *39*, 8173–8186.
7. Tarassov, I., Kamenski, P., Kolesnikova, O., Karicheva, O., Martin, R.P., Krasheninnikov, I.A., and Entelis, N. (2007). Import of nuclear DNA-encoded RNAs into mitochondria and mitochondrial translation. Cell Cycle *6*, 2473–2477.
8. Endo, T., Yamano, K., and Yoshihisa, T. (2010). Mitochondrial matrix reloaded with RNA. Cell *142*, 362–363.
9. Schneider, A. (2011). Mitochondrial tRNA import and its consequences for mitochondrial translation. Annu. Rev. Biochem. *80*, 1033–1053.
10. Yamada, Y., Akita, H., Kamiya, H., Kogure, K., Yamamoto, T., Shinohara, Y., Yamashita, K., Kobayashi, H., Kikuchi, H., and Harashima, H. (2008). MITO-Porter: A liposome-based carrier system for delivery of macromolecules into mitochondria via membrane fusion. Biochim. Biophys. Acta *1778*, 423–432.
11. Yamada, Y., and Harashima, H. (2008). Mitochondrial drug delivery systems for macromolecule and their therapeutic application to mitochondrial diseases. Adv. Drug Deliv. Rev. *60*, 1439–1462.
12. Sato, Y., Sakurai, Y., Kajimoto, K., Nakamura, T., Yamada, Y., Akita, H., and Harashima, H. (2017). Innovative Technologies in Nanomedicines: From Passive Targeting to Active Targeting/From Controlled Pharmacokinetics to Controlled Intracellular Pharmacokinetics. Macromol. Biosci. *17*, 1600179.
13. Sato, Y., Nakamura, T., Yamada, Y., and Harashima, H. (2016). Development of a multifunctional envelope-type nano device and its application to nanomedicine. J. Control. Release *244* (Pt B), 194–204.
14. Ishikawa, T., Somiya, K., Munechika, R., Harashima, H., and Yamada, Y. (2018). Mitochondrial transgene expression via an artificial mitochondrial DNA vector in cells from a patient with a mitochondrial disease. J. Control. Release *274*, 109–117.
15. Yamada, Y., Furukawa, R., Yasuzaki, Y., and Harashima, H. (2011). Dual function MITO-Porter, a nano carrier integrating both efficient cytoplasmic delivery and mitochondrial macromolecule delivery. Mol. Ther. *19*, 1449–1456.
16. Yamada, Y., and Harashima, H. (2012). Delivery of bioactive molecules to the mitochondrial genome using a membrane-fusing, liposome-based carrier, DF-MITO-Porter. Biomaterials *33*, 1589–1595.
17. Wang, G., Shimada, E., Zhang, J., Hong, J.S., Smith, G.M., Teitell, M.A., and Koehler, C.M. (2012). Correcting human mitochondrial mutations with targeted RNA import. Proc. Natl. Acad. Sci. USA *109*, 4840–4845.
18. Khalil, I.A., Kogure, K., Futaki, S., and Harashima, H. (2006). High density of octaarginine stimulates macropinocytosis leading to efficient intracellular trafficking for gene expression. J. Biol. Chem. *281*, 3544–3551.
19. Takano, Y., Munechika, R., Biju, V., Harashima, H., Imahori, H., and Yamada, Y. (2017). Optical control of mitochondrial reductive reactions in living cells using an electron donor-acceptor linked molecule. Nanoscale *9*, 18690–18698.
20. Yamada, Y., Nakamura, K., Abe, J., Hyodo, M., Haga, S., Ozaki, M., and Harashima, H. (2015). Mitochondrial delivery of Coenzyme Q10 via systemic administration using a MITO-Porter prevents ischemia/reperfusion injury in the mouse liver. J. Control. Release *213*, 86–95.
21. Gao, X., and Huang, L. (1996). Potentiation of cationic liposome-mediated gene delivery by polycations. Biochemistry *35*, 1027–1036.
22. Li, S., Rizzo, M.A., Bhattacharya, S., and Huang, L. (1998). Characterization of cationic lipid-protamine-DNA (LPD) complexes for intravenous gene delivery. Gene Ther. *5*, 930–937.
23. Newton, C.R., Graham, A., Heptinstall, L.E., Powell, S.J., Summers, C., Kalsheker, N., Smith, J.C., and Markham, A.F. (1989). Analysis of any point mutation in DNA. The amplification refractory mutation system (ARMS). Nucleic Acids Res. *17*, 2503–2516.

24. Kuznetsov, A.V., Veksler, V., Gellerich, F.N., Saks, V., Margreiter, R., and Kunz, W.S. (2008). Analysis of mitochondrial function in situ in permeabilized muscle fibers, tissues and cells. Nat. Protoc. *3*, 965–976.

25. Mercer, T.R., Neph, S., Dinger, M.E., Crawford, J., Smith, M.A., Shearwood, A.M., Haugen, E., Bracken, C.P., Rackham, O., Stamatoyannopoulos, J.A., et al. (2011). The human mitochondrial transcriptome. Cell *146*, 645–658.

26. Salinas, T., Duchêne, A.M., and Maréchal-Drouard, L. (2008). Recent advances in tRNA mitochondrial import. Trends Biochem. Sci. *33*, 320–329.

27. Russo, A., Russo, G., Cuccurese, M., Garbi, C., and Pietropaolo, C. (2006). The 3′-untranslated region directs ribosomal protein-encoding mRNAs to specific cytoplasmic regions. Biochim. Biophys. Acta *1763*, 833–843.

28. Futaki, S., Ohashi, W., Suzuki, T., Niwa, M., Tanaka, S., Ueda, K., Harashima, H., and Sugiura, Y. (2001). Stearylated arginine-rich peptides: a new class of transfection systems. Bioconjug. Chem. *12*, 1005–1011.

29. Abe, J., Yamada, Y., Takeda, A., and Harashima, H. (2018). Cardiac progenitor cells activated by mitochondrial delivery of resveratrol enhance the survival of a doxorubicin-induced cardiomyopathy mouse model via the mitochondrial activation of a damaged myocardium. J. Control. Release *269*, 177–188.

30. Mizushima, W., Takahashi, H., Watanabe, M., Kinugawa, S., Matsushima, S., Takada, S., Yokota, T., Furihata, T., Matsumoto, J., Tsuda, M., et al. (2016). The novel heart-specific RING finger protein 207 is involved in energy metabolism in cardiomyocytes. J. Mol. Cell. Cardiol. *100*, 43–53.

31. Mazaki, Y., Takada, S., Nio-Kobayashi, J., Maekawa, S., Higashi, T., Onodera, Y., and Sabe, H. (2019). Mitofusin 2 is involved in chemotaxis of neutrophil-like differentiated HL-60 cells. Biochem. Biophys. Res. Commun. *513*, 708–713.